International Journal of Engineering and Technical Research (IJETR)
ISSN: 2321-0869 (O) 2454-4698 (P), Volume-11, Issue-5, May 2021

Modeling of pressure fluctuations in a wellbore while accelerated axial movement of the drillstring

Mejbahul Sarker

Abstract - Oilwell drilling failures are very costly. Axial motion of the drillstring causes severe pressure variations while tripping operations and drilling from floaters. These pressure variations could result in well integrity or well control problems which can be avoided if pressure imbalances are predicted before this operation engaged. To predict these pressure imbalances, number of analytical models have been developed but require time-consuming numerical analysis. One of the key factors in simulation of downhole pressure fluctuations is to have a hydraulics model coupled with drillstring axial motions. This paper demonstrates a vertical oilwell hydrodynamics model containing an axially moving drillstring and drillstring-fluid interaction. Submodel construction and integration was facilitated by use of the bond graph formalism. Overall simulation results show that the model enables to solve the one-dimensional hydraulic behavior of a vertical drilling well, especially pressure fluctuation phenomena which includes heave induced pressure fluctuations. The main contribution of this paper is a model suitable for parametric study of the effect of drillstring axial motions on bottomhole pressure.

Keyword: Drilling, hydrodynamics, drillstring-fluid interaction, lumped segments approach, heave motion, simulation.

1. INTRODUCTION

In drilling operations performed in the oil and gas industry, one of the most important challenges is to control the pressure of the drilling fluid, often called drilling mud. This drilling fluid is pumped at high pressure into the drill string at the top of the well, flows through the drill bit into the well, and continues up the well annulus carrying out to the surface (Fig. 1). In recent years, operators are intensively focusing on deep water exploration due to the limited oil and gas resources in shallow water. The drilling operations requires tight down hole pressure margins [2]. And by improving the pressure control for the drilling operations former undrillable wells becomes drillable. Which will make the oilfields more profitable and extend their life expectancy. It will also make drilling operations safer by preventing kicks and preventing environmental damages caused by mud leaking into the pore space. The deep-water drilling operations require flexibility in mobility from one field to another which is delivered by floating structures such as drillships and semi-submersible drilling units. Semi-submersibles have minimum structures exposed to wave actions and therefore provide a more stable station for drilling operations due to their smaller water-plane areas, and are able to operate in harsher environmental conditions as compared with drillships. Deep water wells are in open seas with considerable harsh environmental conditions.

The heave compensation systems have proved to be an essential component in offshore drilling to minimize the force fluctuation on drillstring and risers [3]. These systems use pneumatic-hydraulic mechanisms to compensate for the heave. One of the most critical phases when drilling from a floating drilling rig in terms of downhole, is pipe connection. During this procedure, the conventional heave compensation is not operational as the drill string is climbed to the drill floor. Consequently, the drill bit functions as a piston creating large pressure variations in the drill bit pressure. Dynamic loads caused by vessel heave are almost entirely transmitted to the drillstring when placed in the slips during non-drilling periods, or when the required compensation loads are greater than the compensator's capacity. When the drill bit moves down into the well the pressure increases (surging), and upward movement decreases the pressure (swabbing). Strong surging and swabbing pressures can cause damage to the well, neighboring wells, personnel, environment or drilling equipment [4].

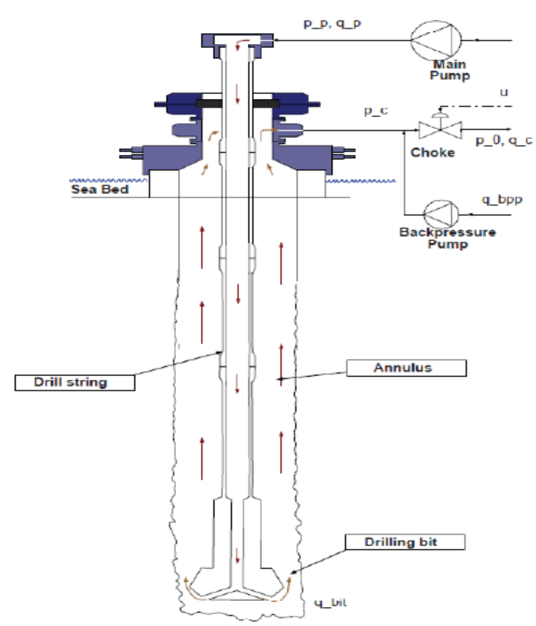

Figure 1: Well and hardware configuration in a managed pressure drilling system [adopted from [1]]

Numerical analysis of the coupled dynamics between the mud flow rate and drillstring velocity has been the focus of describing the flow and pressure fluctuations in the borehole. The estimation of the downhole pressure during managed pressure drilling using a simple three-state model of the hydraulics has been discussed in [5]. This model is too low dimensional to capture transient distributed effects during oscillating string movements.

A higher dimensional mathematical model of well hydraulics based on a finite volume discretization has been proposed in [6]. The model incorporates various MPD operations, including circulating in new mud, vertical motion and rotation of the drill string. Researchers in [7] developed a general dynamic model for any flow related operation during well construction and interventions. The model includes dynamic 2-D temperature calculations, covering the radial area affecting the well and assuming radial symmetry in the vicinity of the well. The approach has more flexibility, improved accuracy, reduced numerical diffusion and increased computational speed. Whereas researchers in [8] presented a model considering the fluid dynamics in the annulus, inside the pipe, and below the it, as well as the drillstring dynamics. The model has been designed for the pipe-tripping and pipe-running operations, where the drillstring velocity is almost constant.

A quantitative theoretical description of surge pressures generated by the pipe movement in a mud-filled wellbore has been developed in [9]. The formulated theory predicted the sequence and magnitudes of the positive and negative surges. The theory of viscous-drag pressure surges has been approximated by simplified graphs and calculation procedures to facilitate ready use in field operations. An exact solution in the frequency domain of the full coupled dynamics of the mud-in-pipe, mud-in-annulus and elastic pipe subsystems have been presented in [10]. The possible occurrence of resonances in each of the subsystems was also discussed. Researchers in [11] evaluated the effect of drill rig motion on the safety of drilling risers using a mathematical model of motion in the frequency domain. The resultant stresses on the riser are validated to ensure the maximum allowable angle of deflection of the riser and that safety margins are not exceeded.

A mathematical model to capture the coupled dynamic response of a semi-submersible in regular and irregular waves where developed numerical models are calibrated using experimental data has been presented in [12]. In another study, the shortcomings of heave compensation systems were recognized, and procedures were recommended to reduce the effect of heave-induced loading on landing operations as a function of drillship resonance period [13]. A ship motion was modeled with a second order 1-DOF model to simulate forced vibration of landing strings. Contrary to other drillstring vibration types, heave-induced dynamics are out of operator control that makes operation decisions in certain sea states difficult. In this study, the effect of heave motion on the drillstring movement and downhole pressure fluctuations has been studied.

This paper is organized as follows. Section 2 describes the proposed heave induced downhole pressure fluctuation simulator. A complete offshore drilling downhole response simulator that allows to predict the effect of drillstring top movement changes on downhole hydraulic responses follows in Section 3. Conclusions are given in Section 4.

II. DESCRIPTION OF PROPOSED COUPLED DYNAMIC MODEL

In this proposed work we consider the case of pressure changes at the bottom of the well under the disturbance from the vertical motion of the drillstring following the heave motion of the floating rig. The dynamic models used in this work use an energy-based method, Bond Graph Theory, which is an unified dynamic system representation language where the connections between multi-disciplinary elements are represented seamlessly and explicitly by power flows. In the vector form, they give concise descriptions of complex systems. An overview of bond graph approach is given in Appx. A. A lumped-segment approach is used to model the drillstring axial dynamics, fluid flow dynamics inside drillstring and annulus. In the lumped segment approach, the system is divided into a series of inertias, interconnected with compliances. The accuracy of the model depends on the number of elements considered; however, in contrast to a modal expansion approach, the analytical model shapes and natural frequencies need not be determined. If a system model is divided into a larger number of elements, then the accuracy of the results will be higher. The behavior will approach that of a continuous system as the number of segments approaches infinity.

2.1 Modeling of drillstring axial dynamics

A total of 21 segments are used in the dynamic model to capture the first eight axial natural frequencies of the whole drillstring. One segment is used for the relatively short Kelly. For both the drill pipe and collar, a total of 10 segments are used in the model. Fig. 2 shows the schematic of the drillstring axial segment model with the FBD of the axial segment of the vertical drillstring and a bond graph model for the axial motions of a drillstring segment is shown in Fig. 3. The axial segment bond graph model shows a mass (I element) and gravity force source (Se element) associated with segment velocity v. Axial compliance and material damping of the segment are modeled by parallel compliance (C) and dissipative elements, the forces of which are functions of the relative velocity (calculated by the 0-junction) of the segment with respect to the adjoining segment. The buoyancy weight of the drillstring segment acts in the longitudinal direction for the case of vertical drilling.

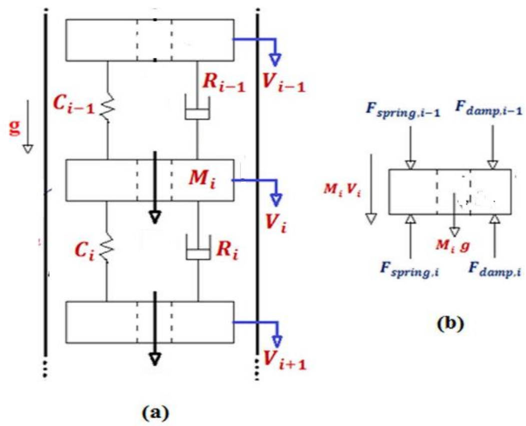

Figure 2: Schematic of (a) drillstring axial lumped segment model and (b) FBD of axial segment.

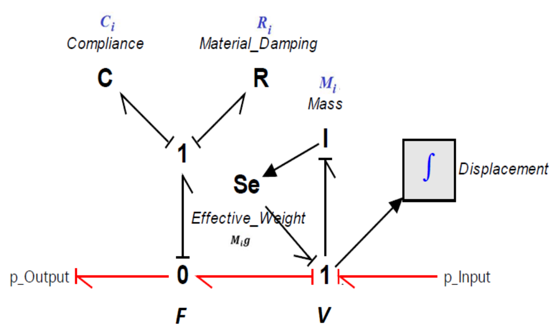

Figure 3: Bond graph model for axial motion of the drillstring segment.

2.2 *Modeling of hydraulic transmission line*

Similarly, a total of 21 segments are used in the dynamic model to capture the fluid flow dynamics inside drillpipe and annulus. The drilling fluid was characterized by the flow rate developed by the mud pumps. Fig. 4 depicts the bond graphs models for the fluid flow segments inside drillpipe and annulus. The segments bond graph models show a fluid inertia (I element) and hydrostatic pressure source (Se element) associated with segment fluid flow velocity *q*. Fluid transmission line compliance of the segment are modeled by compliance (C), the pressures of which are functions of the relative fluid flow velocity (calculated by the 0-junction) of the segment with respect to the adjoining segment.

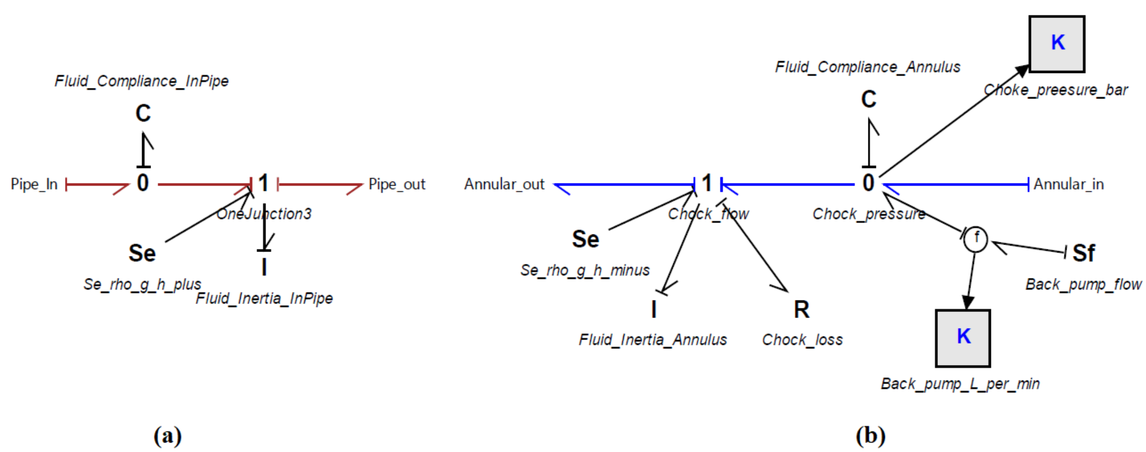

Figure 4: Bond graph dynamics models for (a) fluid flow inside drillstring and (b) fluid flow in annulus.

2.3 *Coupling between drillstring axial movement and fluid flow transmission line*

The coupling model accounts for the effect of drilling fluid circulation in the drillstring and the annular space between the drillstring and the wellbore, on drillstring motions. Nonlaminar Newtonian flow formulations are used in calculation of fluid drag force/damping for the longitudinal motion. Hydrodynamic damping due to drilling fluid circulation in the drillstring and the annular space was considered in the longitudinal direction instead of viscous damping. The equations of the fluid drag forces to the drillstring axial movements are shown in Appx. B. The corresponding bond graph coupling dynamic model is shown in Fig. 5.

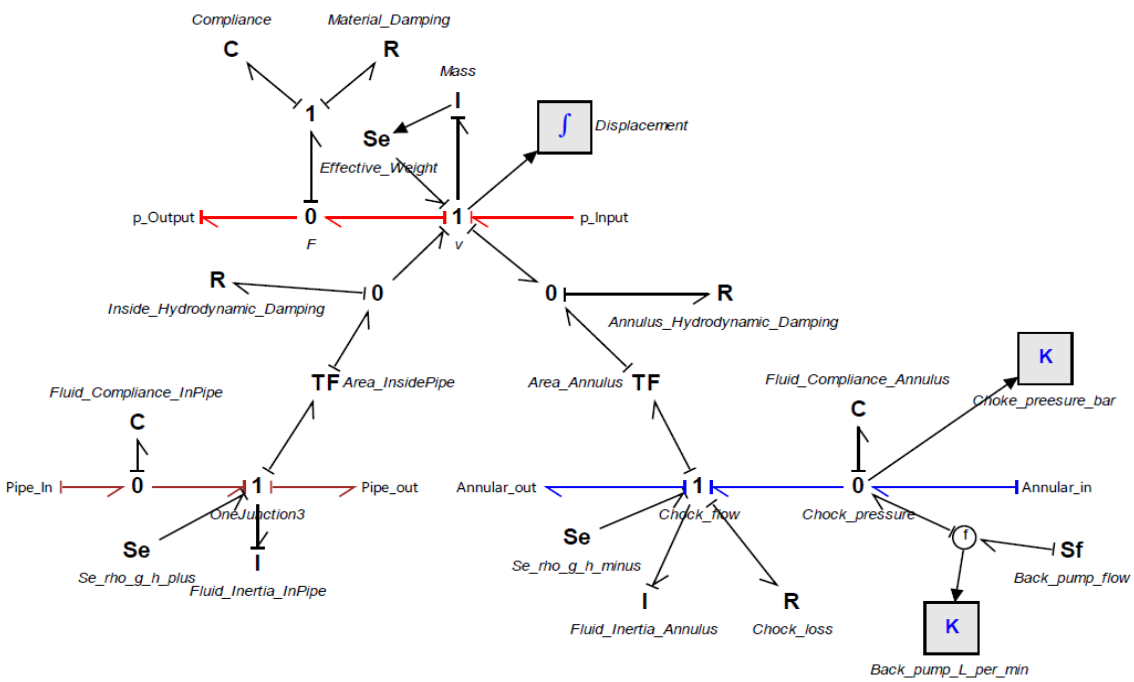

Figure 5: Bond graph coupled model between drillstring axial movement and fluid flow transmission lines.

2.4 Modeling the downhole boundary condition

The bottomhole boundary condition consists the logic of pipe connection phenomena and during connections the pressure in the mud-in-pipe is significantly lower than annulus, the drill bit is fitted with a non-return valve, hence there is no flow through the bit. The bit axial movements transferred into the disturbances in the downhole fluid flow. The bottom-hole momentum balance is developed in the model. A transfer function is used for modeling the bottom-hole momentum balance. The modified logical R element is used to model the non-return valve and it provides a very high resistance for the flow in opposite direction. The pressure losses at the bit nozzles are considered into the model. The bond graph model of the downhole boundary condition is shown in Fig. 6.

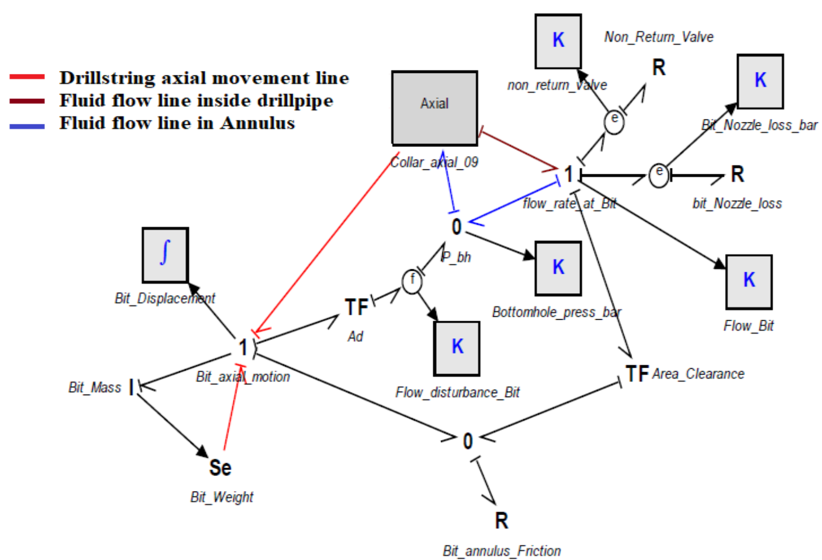

Figure 6: Bond graph model for bottomhole boundary condition.

III. SIMULATION RESULTS

The bond graph model of the offshore drilling system is shown in Fig. C1. Table D1 summarizes all relevant data that is used in the current simulation. The main objective of this simulation is to show the ability of the proposed model to capture the heave induced downhole pressure fluctuation for an offshore drilling system. The model has the capability to simulate the pipe connection condition where the drillstring is attached to the offshore rig floor. The simulation results at the 1750 m measuring depth are shown in Figs. 7-10. The drilling fluid circulation frictional pressure losses inside the drillstring and in the annulus are shown in Fig. 7. The pressure loss increases when the drilling fluid flow rate is increased. The total frictional pressure loss in the annulus is less as compared with the frictional pressure losses inside the drillstring. The simulated frictional pressure losses can be verified with the filed measurement from [5]. The equations used in the model for simulating the frictional pressure losses provide a very accurate prediction thus the model can be an effective tool for the prediction of downhole disturbance.

The abnormal wave velocity plot for the case of severe offshore environment is shown in Fig. 8. The corresponding vertical movement plot at the top of the drillstring shows the high amplitude displacement during the pipe connection. And during the drilling the heave compensators normalized the wave movements. The bit axial velocity plot indicates that the multi modes order model can capture the transmission of disturbance from the top of the drillstring to the bit. The downhole fluid flow disturbance plot in Fig. 8 clearly validates the capability of the model to simulate the downhole coupling boundary condition. The mechanical energy disturbance transfers into the hydraulic excitation at the bottom of the drillstring. The fluid flow disturbance profile is found to be similar to the wave velocity profile for the case of pipe connection. And the drilling fluid flow rate is zero during the drill pipe connection as the top of the drillstring is detached from the top drive and attached to the rig floor. The mud flow rate plot from 330 seconds to 600 seconds in Fig. 9 simulates the pipe connection period for this simulation. The corresponding simulated mud pump pressure plot is shown in Fig. 9. The back pump pressure is always constant to provide a certain fluid flow through the chock. The chock pressure plot shows the similar trend of disturbance found in the heave motion profile. Thus, chock pressure surface measurement can be an effective tool to predict the downhole pressure disturbance.

The model effectively simulates the heave induced bottom hole pressure disturbance shown in Fig. 10. The very severe abnormal sea wave condition provides a very high fluctuation in the bottom hole pressure profile. The magnitude of the bottom hole pressure shows that it can clearly exceed the narrow safe drilling downhole pressure margin (i.e. the window between the pore pressure and fracture pressure) for the case of harsh offshore environment. The corresponding pressure loss at the bit nozzle and the mud flow rate at the non-return valve are shown in Fig. 10. The overall simulation results show that the model is capable to simulate the offshore drilling conditions and can be an effective tool to predict the severe downhole responses. The modeling software platform allows to change the input parameters and provides faster simulation time. Also, the software output platform provides the greater flexibility to plot the necessary responses of the system. The simulation results *(i.e.* data and plots) can be exported and stored for the future analysis. The simulation time can be controlled by changing both the integration methods and step size. In this simulation the Runge Kutta-4 is used as an integration method and the selected 0.0005 step size provides the better dynamic responses.

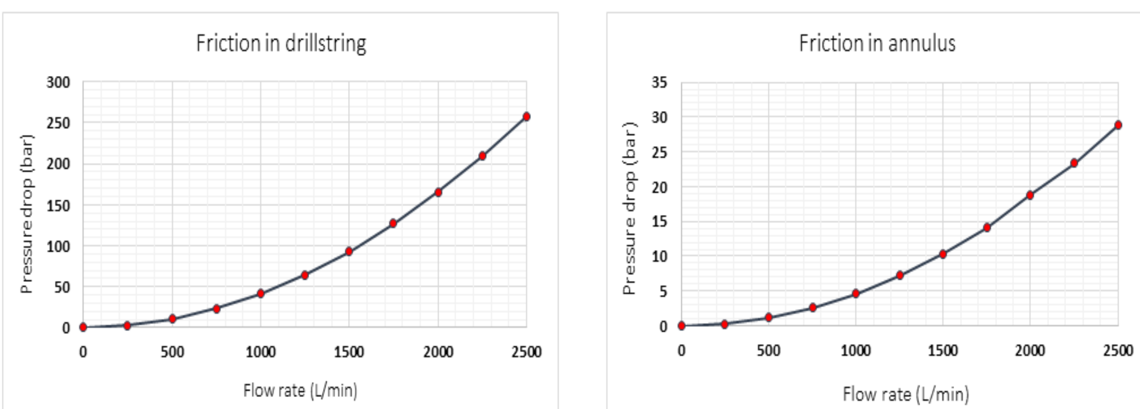

Figure 7: Plots of drilling fluid pressure drops inside drillstring and in annulus due to the friction for 1750 m drilling depth.

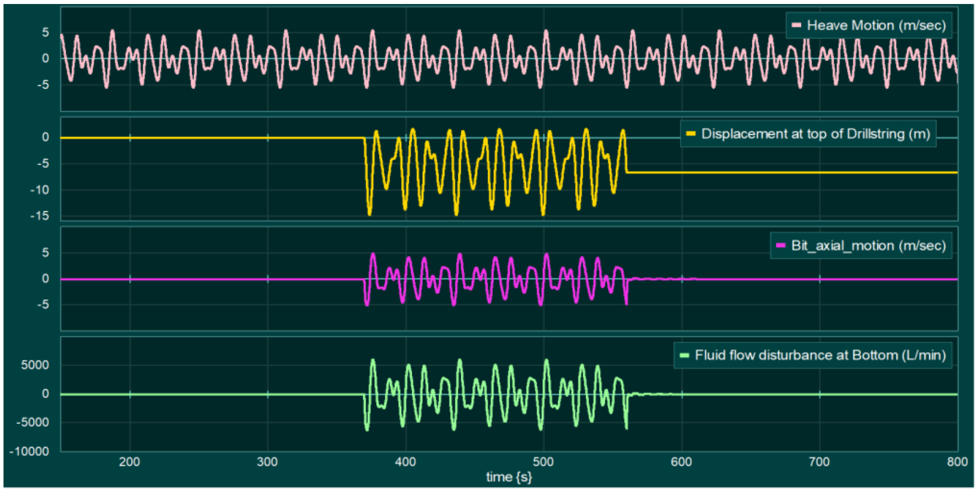

Figure 8: **The heave motion, displacement at the top of the drillstring, bit axial velocity and fluid flow disturbance at downhole for the case of both normal drilling and pipe connection in offshore drilling.**

Figure 9: **The main pump flow rate, back pump flow rate, pressure at the main pump and choke pressure for the case of both normal drilling and pipe connection in offshore drilling.**

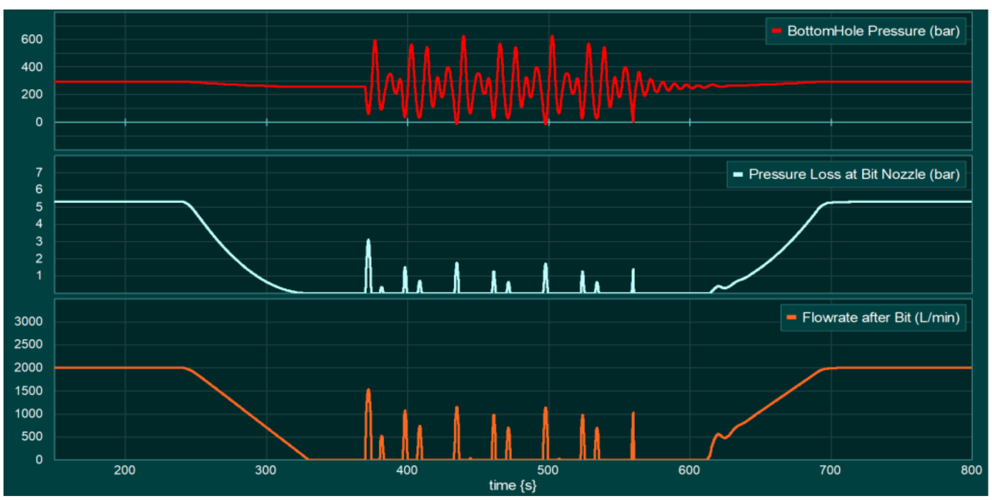

Figure 10: **The bottomhole pressure, pressure loss at the bit nozzle and flow rate after the bit for the case of both the normal drilling and pipe connection in offshore condition.**

IV.CONCLUSIONS

Development of a bond graph model of a vertical offshore drilling system, capturing the drillstring axial movements and the complete fluid flow transmission line dynamics, using lumped parameters approach has been presented. The dynamic model accounts the hydrodynamic damping to capture the coupling friction dynamics between the drillstring axial movements and fluid flow dynamics. The model incorporates a transfer coupling mechanics between the mechanical bit axial movements and downhole fluid flow disturbance. Implementing of the model in 20Sim® commercial software, which allows block diagrams to be superimposed on the bond graphs, greatly facilitated inclusion of the coupled hydrodynamics damping. The simulation time is very fast compared to the high order finite-and discrete-element models, making the model suitable as a tool for design and sensitivity analysis. The frictional pressure losses obtained from the proposed model is in qualitative agreement with the downhole measurement resources. The bit axial velocity and downhole pressure obtained from the simulation results show the model can be a very effective tool for analyzing the effect of severe offshore condition on the drilling downhole responses. The application of an abnormal sea waves to the offshore rig can provide a high amplitude drillstring movements which eventually transmits to the bit in the absence of the heave compensator. The proposed model can be used as a tool for predrilling analysis. The ability to predict the segment axial movements and pressures throughout the string allows for effectively analyzing of dynamic downhole responses. The model provides capabilities for the simulation of a broad suite of problems in the drilling industry including bottom hole pressure design, and drilling efficiency optimizations. The model can be integrated with swab/surge pressures models to simulate bottom-hole conditions for kick control and formation break-down analysis, for instance. It can be used to design the controller for the managed pressure drilling systems.

REFERENCES

[1] Pavlov, A., Kaasa, G.O. and Imsland, L. (2009). “Experimental disturbance rejection on a full-scale drilling rig,” in *Proceedings of IFAC Nonlinear Control Systems Symposium*.

[2] Erivwo, O. and Adeleye, O. (2012). Narrow Margin Drilling in Deepwater: Solution Concepts. *Presented at the SPE Deepwater Drilling and Completions Conference*, Galveston, Texas, USA. June 20-21.

[3] Woodall-Mason, N. and Tilbe, J. (1976). Value of Heave Compensators to Floating Drilling. *Society of Petroleum Engineers*. Doi:10.2118/5267-PA.

[4] Huang, L., Tahchiev, G.V. and Cao, Y. (2011). Investigation of Drill Bit Heave Response to Drill Rig Heave Excitation. *International Society of Offshore and Polar Engineers*.

[5] Kaasa, G.O., Stamnes, Q.N., Aamo, O.M. et al. (2012). Simplified Hydraulics Model Used for Intelligent Estimation of Downhole Pressure for a Managed Pressure Drilling Control System. *SPE Drill & Compl*, 27(1):127-138. SPE 143097-PA.

[6] Landet, I. S., Mahdianfar, H., Pavlov, A. et al. (2012). Modeling for MPD Operations with Experimental Validation. *Presented at the IADC/SPE Drilling Conference and Exhibition*, San Diego, California, 6–8 March. SPE-150461-MS. https://doi.org/10.2118/150461-MS.

[7] Petersen, J., Rommetveit, R., Bjorkevoll, K. S. et al. (2008). A General Dynamic Model for Single andMulti-phase Flow Operations during Drilling, Completion, Well Control and Intervention. Presented at the *IADC/SPEAsia PacificDrilling Technology Conference and Exhibition*, Jakarta, 25–27 August. SPE-114688-MS. https://doi.org/10.2118/114688-MS.

[8] Mitchell, R. (1988). Dynamic Surge/Swab Pressure Predictions. *SPE Drill Eng*, 3(3): 325–333. SPE-16156-PA. https://doi.org/10.2118/16156-PA.

[9] Burkhardt, J. A. (1961). Wellbore Pressure Surges Produced by Pipe Movement. *J Pet Technol*, 13 (6): 595–605. SPE-1546-G-PA. https://doi.org/10.2118/1546-G-PA.

[10] Aarsnes, U. J. F., Gleditsch, M. S., Aamo, O. M. et al. (2014). Modeling and Avoidance of Heave-Induced Resonances in Offshore Drilling. SPE Drill & Compl 29 (4): 454–464. SPE-173178-PA. https://doi.org/10.2118/173178-PA.

[11] Arda, E.B. Djatmiko, Murdjito. (2012). “A Study on the Effect of Semi-Submersible Drilling Rig Motions with Variation in Mooring Line Pre-Tension to the Safety of Drilling Riser”, 8th *International Conference on Marine Technology*, At Kuala Terengganu, Malaysia, 20 – 22 October,Volume: I.

[12] Kurian, V. J., Yassir, M. A. and Harahap, I. S. (2010). “Nonlinear Coupled Dynamic Response of a Semi-submersible Platform”. *International Society of Offshore and Polar Engineers*.

[13] Everage, S. D., Zheng, N. and Ellis, S. E. (2005). “Evaluation of Heave-Induced Dynamic Loading on Deepwater Landing Strings”. *Society of Petroleum Engineers*. doi:10.2118/87152-PA.

Mejbahul Sarker
Lecturer, Department of Petroleum Engineering, American University of Kurdistan.

Appendix A

An overview of bond graph formalism

Bond graph is an explicit graphical tool for capturing the energetic structure of a physical system and uniquely suited to the understanding of physical system dynamics. Because of the ability to provide concise description of complex systems the bond graph formulation can be used in hydraulics, mechatronics, thermodynamic and electric systems. The bond graph language expresses a general class of physical systems through power (effort and flow) interactions and the factors of power have different interpretations in different physical domains.

Table A1 expresses the generalized power (effort and flow) variables and energy (momentum and displacement) variables in some physical domains. The generalized inertias and capacitance in bond graph [40] store energy as a function of the system state variables, the sources provide inputs from the environment, and the generalized resistors remove energy from the system. The state variables are generalized momentum and dis-placement for inertias and capacitances, respectively. Where the time derivatives of generalized momentum p and displacement q are generalized effort *e* and flow *f*. The power-conserving elements allow changes of state to take place. Such elements include power-continuous generalized transformer (TF) and gyrator (GY) elements that algebraically relate elements of the effort and flow vectors into and out of the element. In certain cases, such as large motion of rigid bodies in which coordinate transformations are functions of the geometric state, the constitutive laws of these power-conserving elements can be state modulated. Dynamic force equilibrium and velocity summations in rigid body systems are represented by power-conserving elements called 1 and 0 junctions, respectively.

Table A1: Generalized bond graph quantities

Variable	General	Translation	Rotation
Effort	$e(t)$	Force	Torque
Flow	$f(t)$	Velocity	Angular Velocity
Momentum	$p=\int e\,dt$	Linear momentum	Angular momentum
Displacement	$q=\int f\,dt$	Displacement	Angular displacement
Energy	$E(p)=\int^{p} f\,dp$	Kinetic potential	Kinetic Potential
	$E(q)=\int^{q} e\,dq$		

Table A2: Bond graph elements

	SYMBOL	CONSTITUTIVE LAW (LINEAR)	CAUSALITY CONSTRAINTS
SOURCES			
Flow	Sf $\vdash\!\rightharpoonup$	f = f(t)	fixed flow out
Effort	Se $\rightharpoonup\!\mid$	e = e(t)	fixed effort out
ENERGETIC ELEMENTS			
Inertia	$\rightharpoonup\!\mid$ I $\vdash\!\rightharpoonup$ I	$f=\frac{1}{I}\int e\,dt$ $e=I\frac{df}{dt}$	preferred integral
Capacitor	$\vdash\!\rightharpoonup$ C $\rightharpoonup\!\mid$ C	$e=\frac{1}{C}\int f\,dt$ $f=C\frac{de}{dt}$	preferred integral
Resistor	$\vdash\!\rightharpoonup$ R $\rightharpoonup\!\mid$ R	$e=Rf$ $f=\frac{1}{R}e$	none

	SYMBOL	CONSTITUTIVE LAW (LINEAR)	CAUSALITY CONSTRAINTS
2-PORT ELEMENTS			
Transformer	$\xrightarrow{1}\!\mid$ TF $\xrightarrow{2}\!\mid$ n	$e_2 = n\,e_1$ $f_1 = n\,f_2$	effort in – effort out, or flow in – flow out
Modulated Transformer	$\downarrow\theta$ $\xrightarrow{1}\!\mid$ MTF $\xrightarrow{2}$ n(θ)	$e_2 = n(\theta)\,e_1$ $f_1 = n(\theta)\,f_2$	
Gyrator	$\vdash\!\xrightarrow{1}$ GY $\xrightarrow{2}\!\mid$ n	$e_2 = n\,f_1$ $e_1 = n\,f_2$	flow in – flow out, or effort in – effort out
Modulated Gyrator	$\downarrow\theta$ $\vdash\!\xrightarrow{1}$ MGY $\xrightarrow{2}\!\mid$ n(θ)	$e_2 = n(\theta)\,f_1$ $e_1 = n(\theta)\,f_2$	
CONSTRAINT NODES			
1-junction	$\xrightarrow{1}\!\mid$ 1 $\xrightarrow{2}\!\mid$ 3	$e_2 = e_1 - e_3$ $f_1 = f_2$ $f_3 = f_2$	one flow input

Appendix B
EQUATIONS USED IN THE MODEL

FLUID DRAG FORCE/DAMPING FOR COUPLING MODEL

Assuming the nonlaminar Newtonian flow formulations and ignoring any eccentric location of the drillstring in the wellbore, the pressure drop in the annulus between the borehole and a stationary drillpipe can be written as below

$$\Delta P = \frac{\alpha_a \, \rho_m \, Q^2 \, dx}{4 \, \pi^2 \, (r_w - r_0) \, (r_w^2 - r_0^2)^2} \qquad (B1)$$

The resulting longitudinal force, F_A (positive down) exerted on the drillstring segment which is moving with velocity, V_n can be written as below

$$F_A = -\left\{\frac{\alpha_a \, \rho_m \, \pi \, (r_w + r_0) \, dx}{4}\right\} \left| \left[\frac{Q}{\pi \, (r_w^2 - r_0^2)}\right] + V_n \right| \left\{ \left[\frac{Q}{\pi \, (r_w^2 - r_0^2)}\right] + V_n \right\} \qquad (B2)$$

And the drag force on the drillstring due to flow in the drillpipe is given by [8]

$$F_p = -\left\{\frac{\alpha_p \, \rho_m \, \pi \, r_i \, dx}{4}\right\} \left| \frac{Q}{\pi \, r_i^2} - V_n \right| \left\{ \frac{Q}{\pi \, r_i^2} - V_n \right\} \qquad (B3)$$

Appendix C

Bond Graph Model of the System

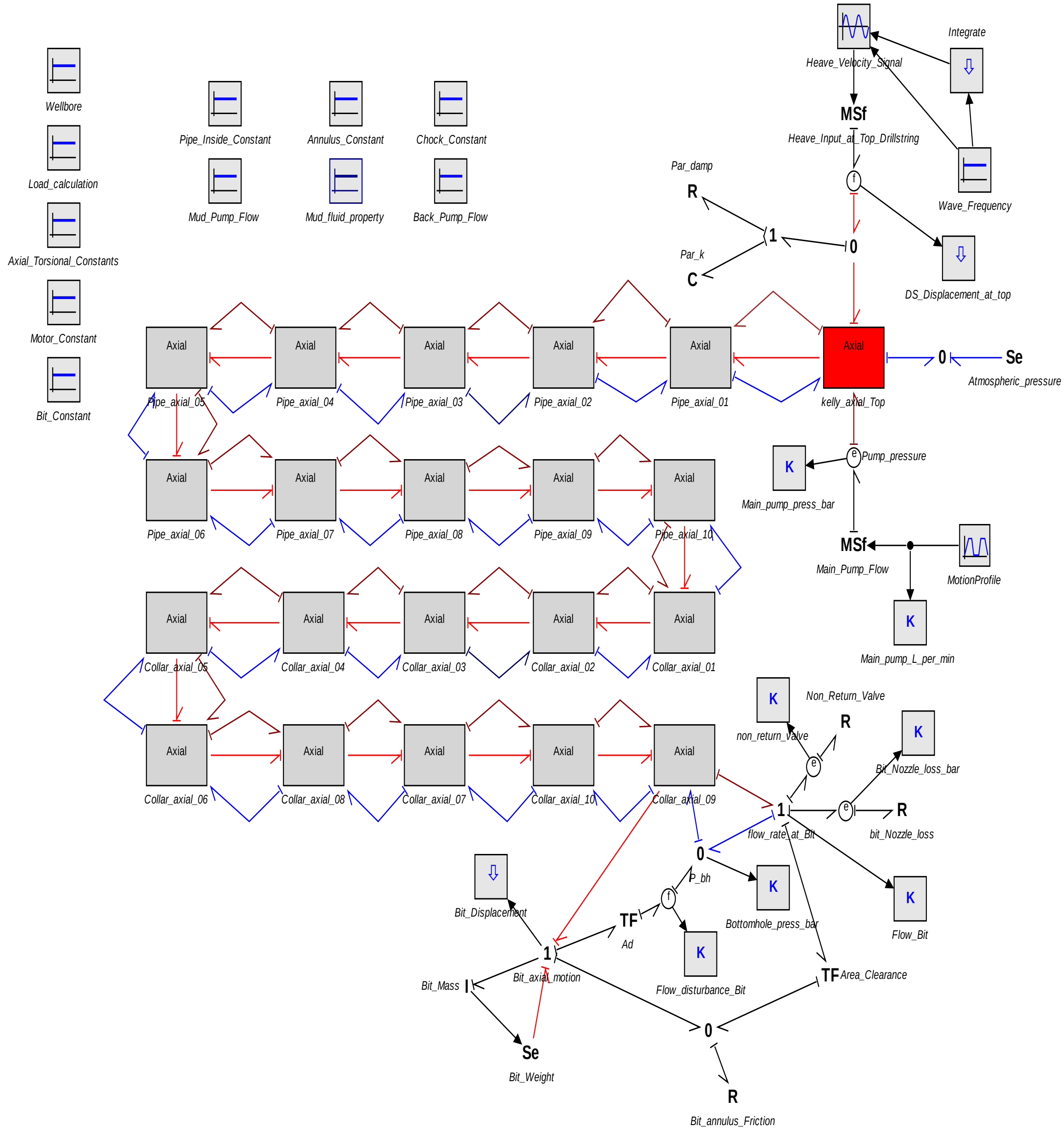

Figure 11: Bond graph model of the system.

International Journal of Engineering and Technical Research (IJETR)
ISSN: 2321-0869 (O) 2454-4698 (P), Volume-11, Issue-5, May 2021

Appendix D

Simulation data

Table D1.
Data used in oilwell drilling simulation.

Drillstring data	
Cable and derrick spring constant	9.3e+06 N/m
Swivel and derrick mass	7031 kg
Kelly length	10 m
Kelly outer diameter	0.379 m
Kelly inner diameter	0.0825 m
Drill pipe length	1540 m
Drill pipe outer diameter	0.101 m (4 in)
Drill pipe inner diameter	0.0848 m (3.34 in)
Drill collar length	200 m
Drill collar outer diameter	0.171 m (6.75 in)
Drill collar inner diameter	0.0571 m (2.25 in)
Drill string material	Steel
Wellbore diameter	0.2 m
Hydraulic data	
Mud fluid density	1198 kg/m^3
Mud flow rate, Q	$Q_m + Q_a \sin(qt)$
Mean mud flow rate, Q_m	0.022 m^3/sec
Mud flow pulsation amplitude, Q_a	0.002 m^3/sec
Freq. of variation in mud flowrate, q	25.13 rad/sec
Equivalent fluid viscosity for fluid resistance to rotation μ_e	30e-03 Pa.sec
Weisbach friction factor outside drill pipe or collar, α_a	0.045
Weisbach friction factor inside drill pipe or collar, α_p	0.035